Ryssänlampi magnetic survey using Radai's UAV system in winter conditions

Detailed Survey Report

20.4.2016

Markku Pirttijärvi & Christian Wieser

Radai Oy

radai

GEOPHYSICAL SURVEYS AND REMOTE SENSING WITH UAV'S

Contents

1. Introduction

In winter 2016 Radai Oy carried out a geophysical magnetic survey at Ryssänlampi site using an unmanned aerial vehicle (UAV). The measurements were commissioned by Geological Survey of Finland (GTK) as a part of UAV-MEMO project funded by Tekes (Finnish Funding Agency for Innovation and Technology) and four mining companies operating in Finland (AA Sakatti Mining, Agnico-Eagle, Mawson, Nordkalk). The purpose of the survey was to 1) re-assess the status of Radai's updated measurement system and 2) to investigate the effect of winter conditions on an UAV based magnetic surveying system.

This detailed survey report describes Radai's magnetic UAV system, the magnetic survey conducted at the Ryssänlampi site, the raw data, data processing steps and the results (total magnetic field) derived from data processing and equivalent layer modelling. It also shows comparisons to Radai's earlier UAV based magnetic data from Ryssänlampi (measured in summer 2015) and GTK's airborne and ground magnetic data and discusses the meaning of the results.

2. Radai's UAV based survey system

Radai's magnetic measurement system is installed into a custom-made UAV (Terrain Scout). The magnetic field is measured by a digital 3-component fluxgate magnetometer. The X, Y, and Z components of the magnetic field are recorded with the data logger combined with Radai's own measurement device. The measurement device also records the GPS time and position (latitude and longitude), UAV orientation (roll, pitch and yaw), and barometric pressure. The accuracy of the GPS positioning is about ±2 m during flight. Technical information on Radai's UAV system is given in Table 1. The UAV is illustrated in Figure 2.1.

After take-off the flight is controlled by an autopilot that follows predefined waypoints. The flight performance is controlled by PC software via a telemetry (radio) link in real time. The same PC software is

used to download the waypoints to the autopilot. Vertical landing system (VLS) prevents damages in UAV landing and SMS based service enables locating the UAV in case of an unwanted crash landing.

Base station near the mobile telemetry/control station measures the temporal variation of the magnetic field and barometric pressure. The intensity of total magnetic field is measured with a proton precession magnetometer. Additionally, a 3-component fluxgate magnetometer, similar to that in the UAV, can be used for base station measurements thus providing variation of individual magnetic field components.

Table 1: Technical information on Radai's UAV system

UAV parameters	**Value**
Electric engine	780 W
Wingspan	2.12 m
Mass	3.6 kg
Payload	1-1.5 kg
Flight speed	10-25 m/s
Flight time	up to 1 h
UAV magnetometer	**Fluxgate**
Noise level	±0.5 nT
Dynamic range	±65 μT
Sampling frequency	10 Hz
Base station magnetometer	**Proton precession**
Resolution	±0.1 nT
Dynamic range	30-60 μT
Sampling frequency	>1 Hz

Figure 2.1. Radai's Terrain Scout UAV.

3. Ryssänlampi magnetic survey

The survey site is located in Northern Finland about 35 km east of Rovaniemi. The red rectangle in Figure 3.1 depicts the survey area defined by GTK. The ETRS-TM35FIN coordinates of the four corner points of the survey area are: (468090, 7375905), (468762, 7376577), (469893, 7375446) and (469221, 7374774). The total area of the survey site is 1.53 km^2 and the direction of the c. 1 km long lines is along SW-NE. The line spacing was made 30 m instead of 50 m used in the earlier survey in summer 2015. Please, note that ETRS-TM35FIN coordinates are used throughout this report, and the DEM data and the background maps are provided by the National Land Survey of Finland.

The magnetic survey was carried out in three campaigns: C1) Feb 12-13 2016, C2) March 5-6 2016 and C3) March 26 2016. Campaigns C1 and C2 were conducted using BVLOS (Beyond Visual Line of Sight) mode with the permission given by TRAFI (the Finnish Transport Safety Agency). Christian Wieser was the principal pilot and safety officer in all campaigns. Ari Saartenoja, Arto Karinen and Markku Pirttijärvi were co-pilots in campaign C3 that was made using EVLOS (Extended Visual Line of Sight) mode. In C3 the communication between the pilot and the co-pilots was established using walkie-talkies.

The final magnetic data of the UAV survey was taken from three separate flights of the last two campaigns (flight F1 from C2 and flights F2 and F3 from C3). The waypoints and the true flight paths are plotted in Figure 3.1. The diamond, circle and triangle shaped symbols and the red, green and blue lines represent the waypoints and true path of flights F1, F2 and F3, respectively. The altitude of the waypoints was designed to follow the topography at the height of 30 m using the digital elevation model (DEM) of the survey area (10 m by 10 m grid). Radai's previous UAV survey was made using a nominal flight height of 40 m.

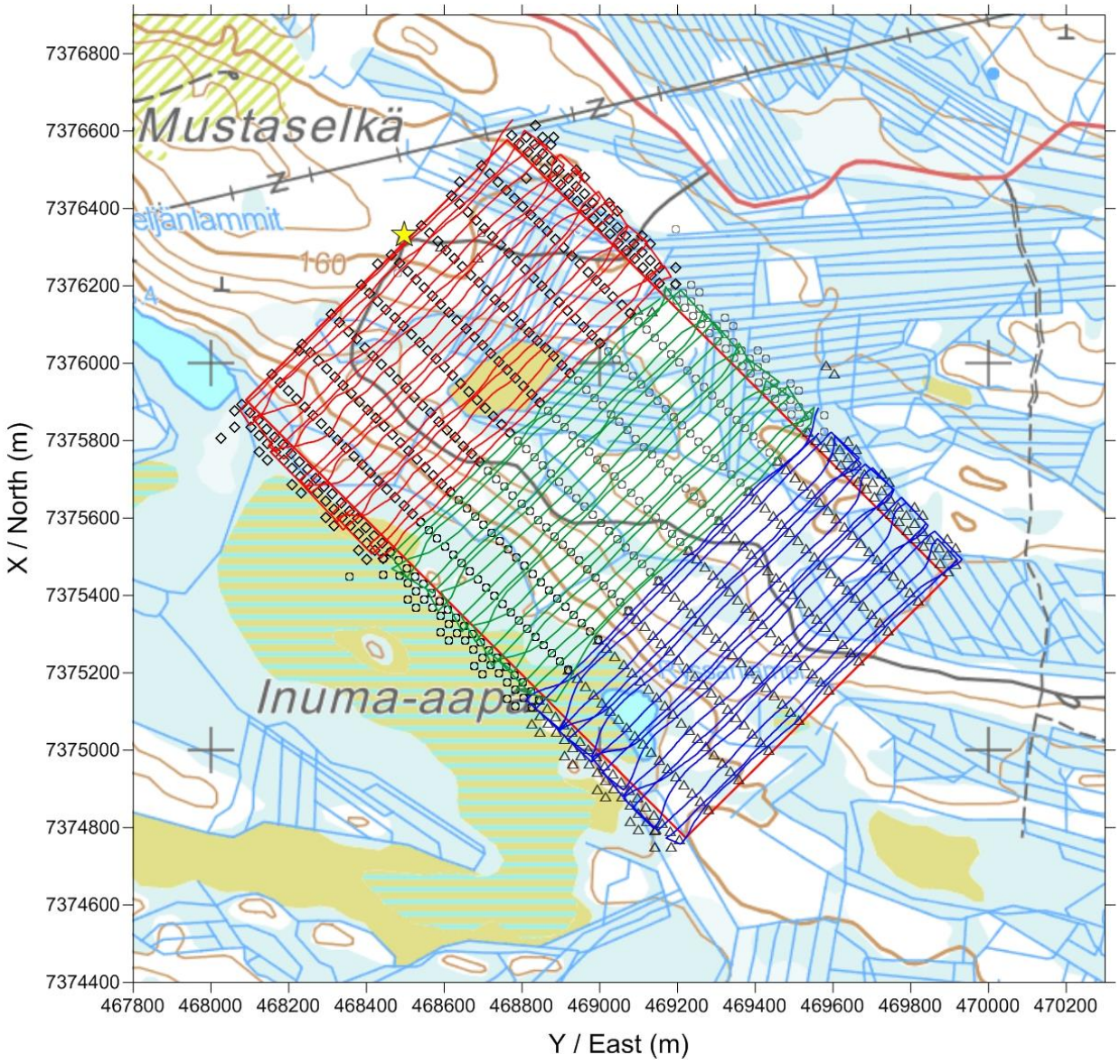

Fig. 3.1. Waypoints designed for Ryssänlampi survey (symbols) and the location of the true flight lines (red, green and blue lines). The red rectangle depicts the borders of the survey area. The yellow start depicts the location of the base/control station. Background map by National Land Survey of Finland © 2014.

Because of the fine line spacing of 30 m, the flight lines were designed so that every second line from NW to SE were measured first (e.g. lines 1,3,5,7,9) and the remaining lines (e.g. lines 8,6,4,2) were measured when returning back towards the base station (the yellow star in Fig. 3.1). The distance between the waypoints was 100 m.

Fig. 3.1 shows that the maximum gap between the true flight lines is about 75 m, which is 150% over the nominal line spacing of 30 m. The maximum gap is of the same size as in Radai's survey from summer 2015 that made using 50 m line spacing. Considering that 50% stray is often considered acceptable and that 75 m is 50% over the nominal line spacing of 50 m, it appears that the UAV is incapable of following the waypoints designed for line separation less than 50 m. The inaccuracy of flight paths is partially affected by the wind and gusts, and partially, the greater speed of the UAV that was needed to account for the increased weight of extra batteries.

Maps of the measured and pre-processed data are shown in Figs. 3.2-3.6. Figure 3.2 shows the UAV orientation. The meaning of the orientation parameters, roll, pitch and yaw, is illustrated in Figure 3.7. Roll becomes visible when the UAV turns from one line to another. Pitch shows up when the UAV descends or ascends due to terrain topography. Yaw is mostly 35 or 145 degrees because the light lines are directed towards NE or SW. The level difference in the roll component of flight F2 (cf. Fig. 3.2) is due to the misalignment of the measurement device containing the orientation sensor.

Because of a bad instrument, barometric pressure could not be obtained for flight F1. Therefore, the flight height was given a constant value equal to the nominal altitude of 30 m (cf. Fig. 3.2).

Because the raw magnetic data (Fig. 3.4) are defined on the reference frame of the UAV, the raw XYZ components are almost useless before the data are rotated using measured roll, pitch and yaw angles. Although the corrected data (Fig. 3.5) and especially the vertical component correlate with the geology, it contains lots of stripe-like artefacts (particularly flight F2). This indicates a mismatch between the true orientation (up, east, north) and the (corrected) orientation of the sensor. In this case the mismatch is not a problem, because the objective was to measure the intensity of the magnetic total field. Recovering the individual XYZ components of the magnetic field would have required more accurate preparations. Please, note that the corrected total field data (Fig. 3.6) include fluxgate calibration and orientation correction, but base station correction has been made only for flight F1.

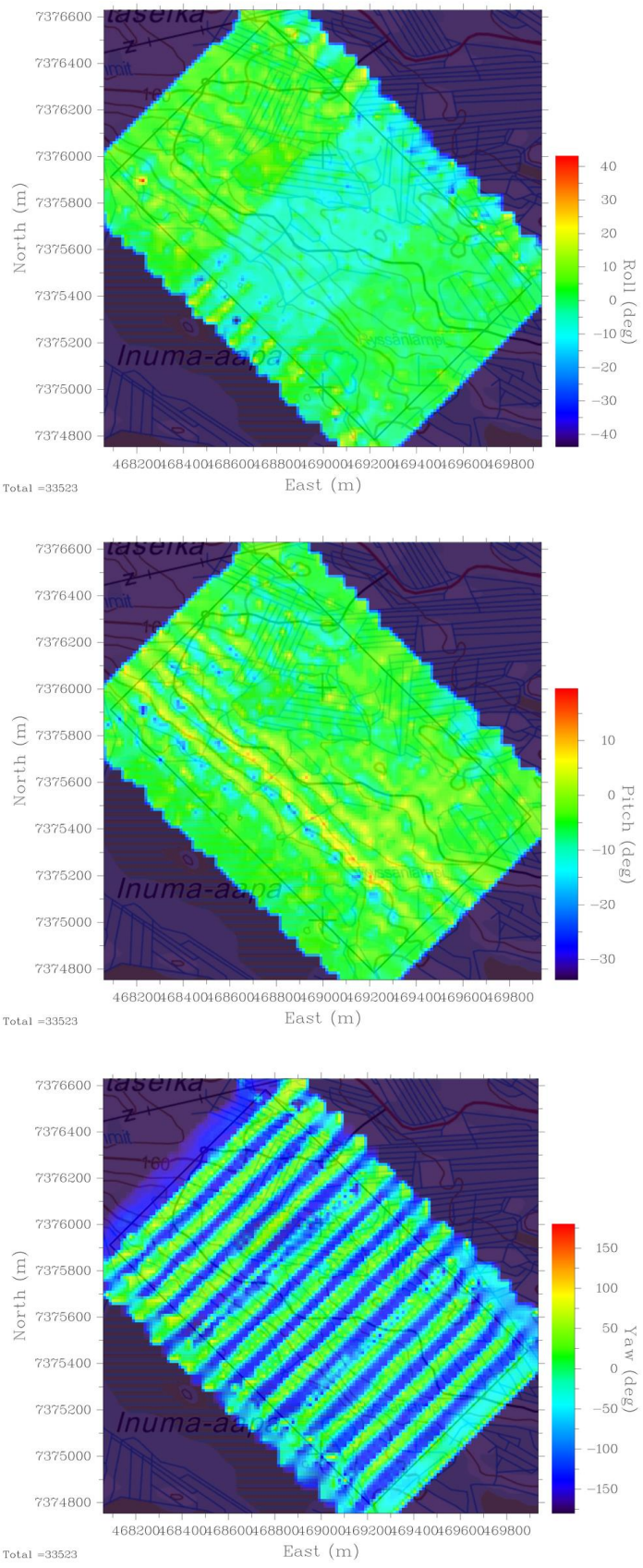

Figure 3.2. Roll, pitch and yaw from Ryssänlampi survey.

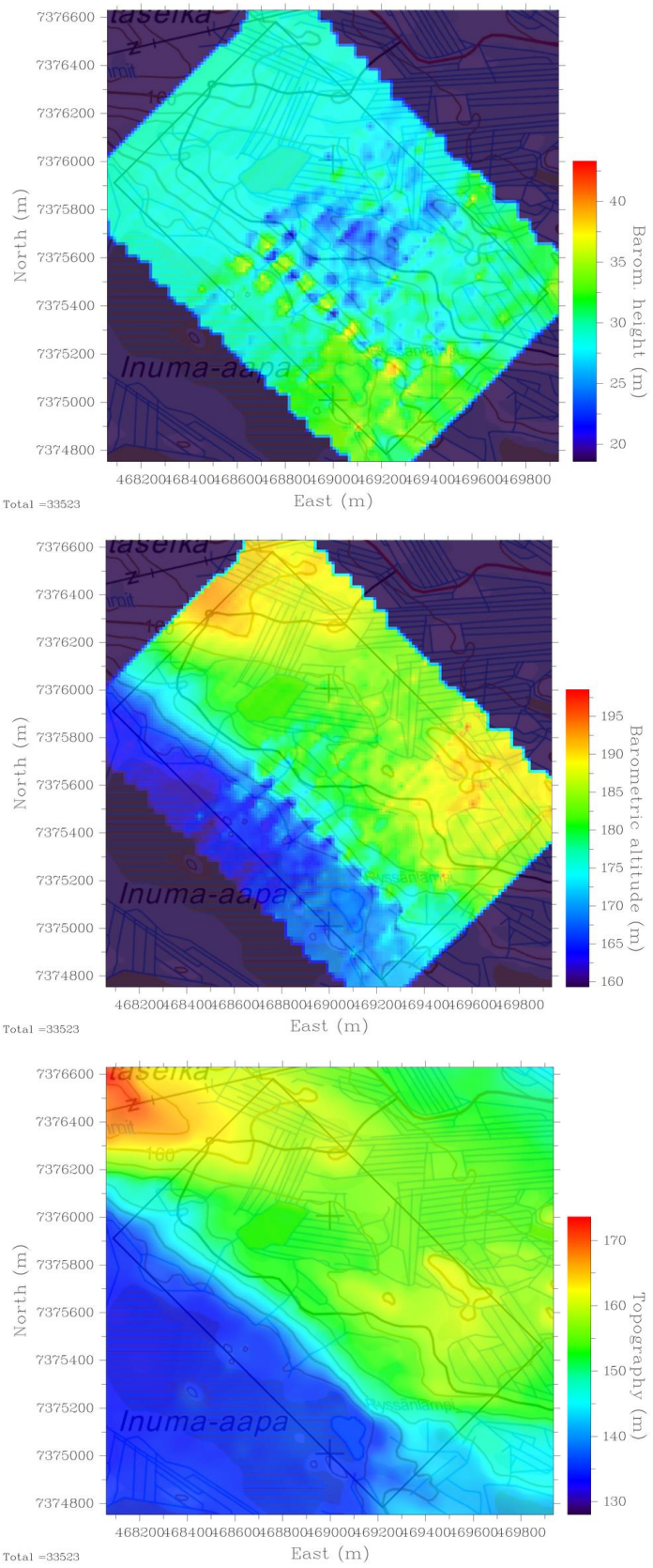

Figure 3.3. Height (from ground), altitude (from sea level) and DEM topography from Ryssänlampi survey.

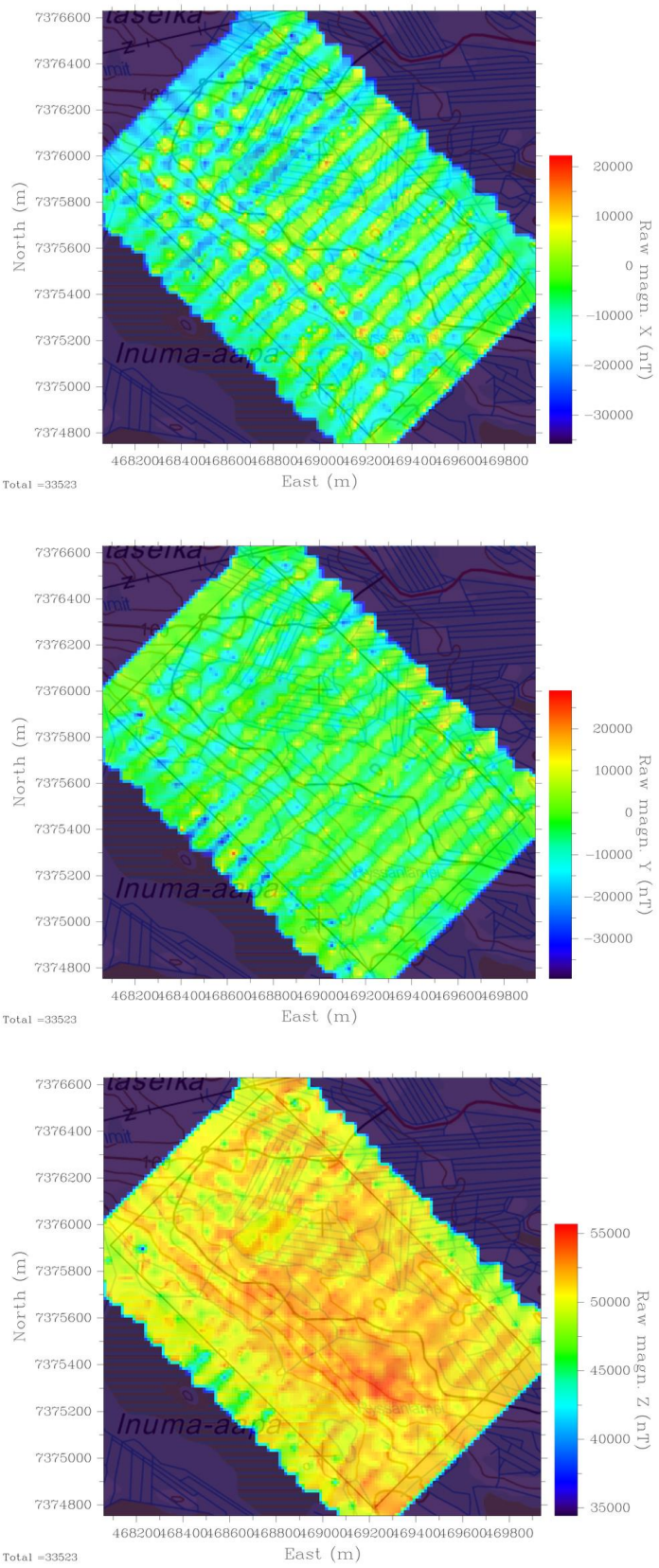

Figure 3.4. Raw magnetic X, Y and Z data components from Ryssänlampi survey.

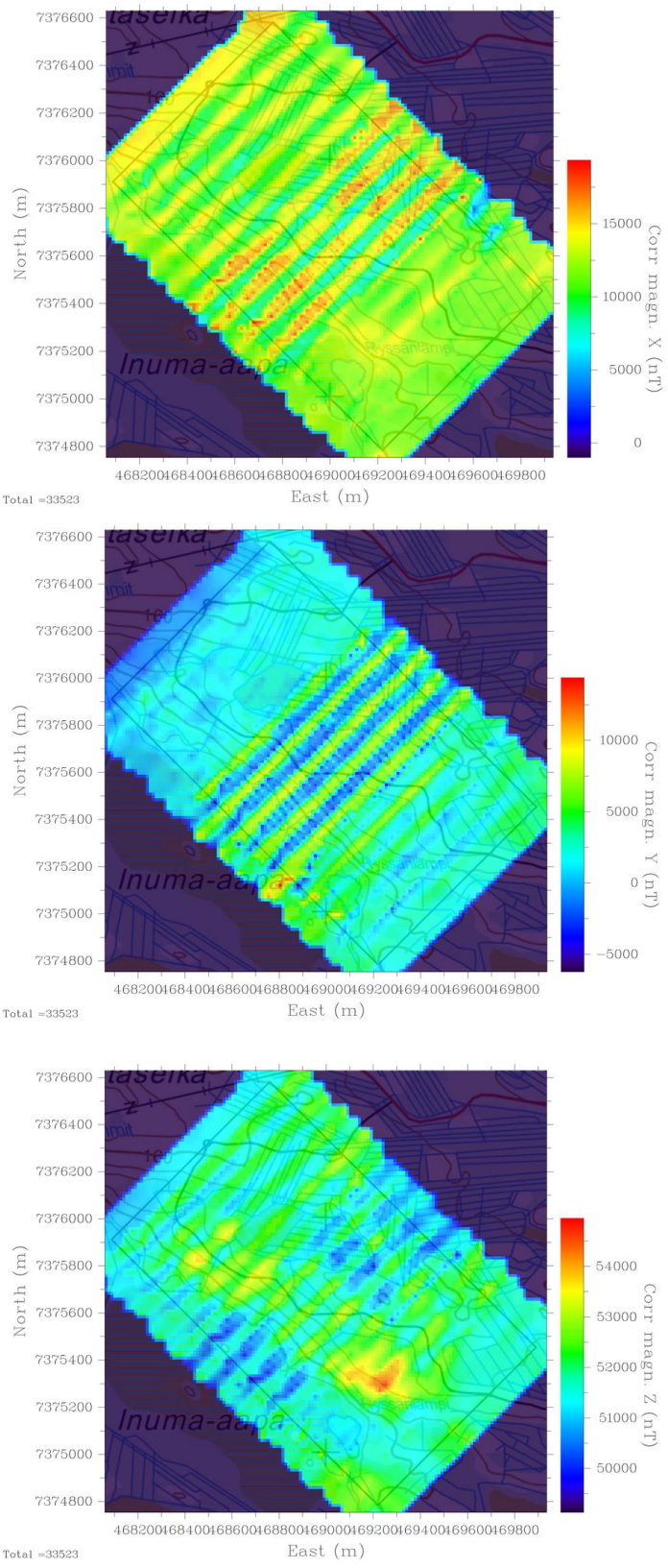

Figure 3.5. Corrected magnetic X, Y and Z data components from Ryssänlampi survey.

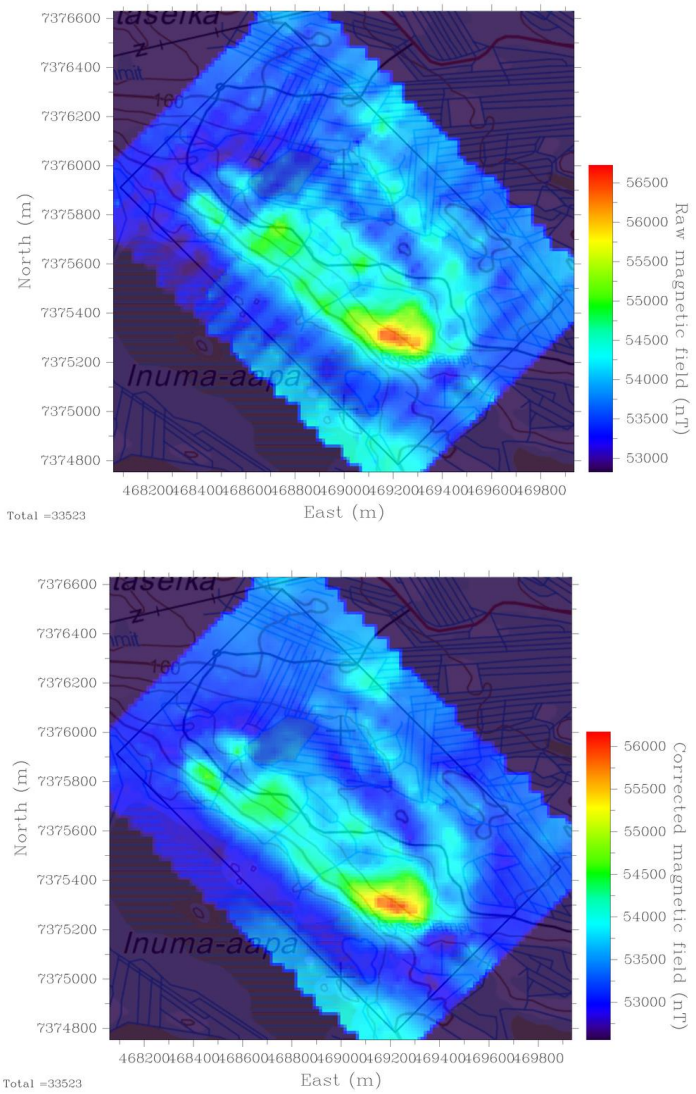

Figure 3.6. Maps of raw and corrected total magnetic field from Ryssänlampi survey.

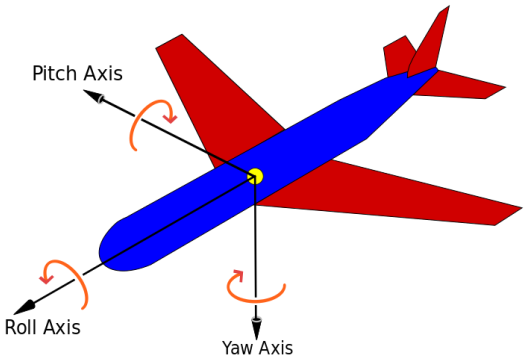

Figure 3.7. Definition of roll, pitch and yaw (https://en.wikipedia.org/wiki/Flight_dynamics_(fixed-wing_aircraft)).

4. Data processing

The data processing was made with RadaiPros software by Dr. Markku Pirttijärvi. The basic data processing steps that are executed on the raw data are listed below.

1. Removal of dummy/missing data values.
2. Removal/averaging of points with identical coordinates.
3. Verification of all angle, pressure and time values.
4. Computation of barometric height from pressure data.
5. Computation of rectangular X and Y coordinates (ETRS-TM35FIN or UTM).
6. Computation of profile distance coordinate and azimuth/heading angle.
7. Application of fluxgate calibration parameters (derived from a separate calibration measurement).
8. Correction of magnetic X, Y, Z components for UAV orientation (roll, pitch and yaw).
9. Computation of the corrected total magnetic field.
10. GPS lag correction (not used because test measurement was not made).
11. Computation of IGRF reference values (B_x, B_y, B_z, B_{tot}, inclination and declination).

After basic processing, each dataset was manually edited and unnecessary points (e.g. when the UAV travels to the survey area and away from there) and turn-around points were removed. Low-pass filtering was made using a wave length of about 40 m (10 samples). After data editing, the total number of data points was 33523, total profile length was 65.1 km and the mean velocity was 13.6 m/s. More statistical information on the survey is given in Table 2. The estimates of the total magnetic field (B_{tot}) are given for the corrected data.

Table 2. Flight statistics on Ryssänlampi magnetic survey

Parameter	Flight F1	Flight F2	Flight F3	Total
Points	12647	10588	10288	33523
Length (m)	22226	21863	21013	65103
Fly-time (min)	29.5	26.1	24.0	79.6
Mean speed (m/s)	12.6	14.0	14.6	13.6
Mean sampling (m)	1.8	2.1	2.0	1.9
Mean height (m)	28.8	27.9	30.9	29.2
Min B_{tot} (nT)	52774	52615	52559	52559
Max B_{tot} (nT)	54762	54830	56172	56172
Mean B_{tot} (nT)	53325	53493	53510	53435

The calibration of the fluxgate sensor is based on the method described in Merayo et al. (2000). The rotation of the measured magnetic field components is not important when dealing with total field data. Determination of the flight altitude is based on barometric pressure and digital elevation models (DEM's). The reference point is located near the base station where the UAV system is initialized before the take-off. Topographic DEM data provided by the National Land Survey of Finland is used to compute the actual height from the ground and the altitude from sea-level for each data point.

The base station data is used to account for the changes in the magnetic field and pressure during the survey. The sampling frequency was 0.1 Hz. Unfortunately, due to a human error the proton precession magnetometer data could not be used at all and the total field derived from fluxgate magnetometer could

be for flight F1 only. Fig. 4.1 shows that magnetic field was very quiet during flight F1 on March 5th 2016. The magnetic field was pretty quiet also on March 26 when flights F2 and F3 were conducted. Figure 4.2 shows that the magnetic field variations on March 26 were about ±20 nT at Sodankylä Geophysical Observatory which is located about 150 km north from Ryssänlampi.

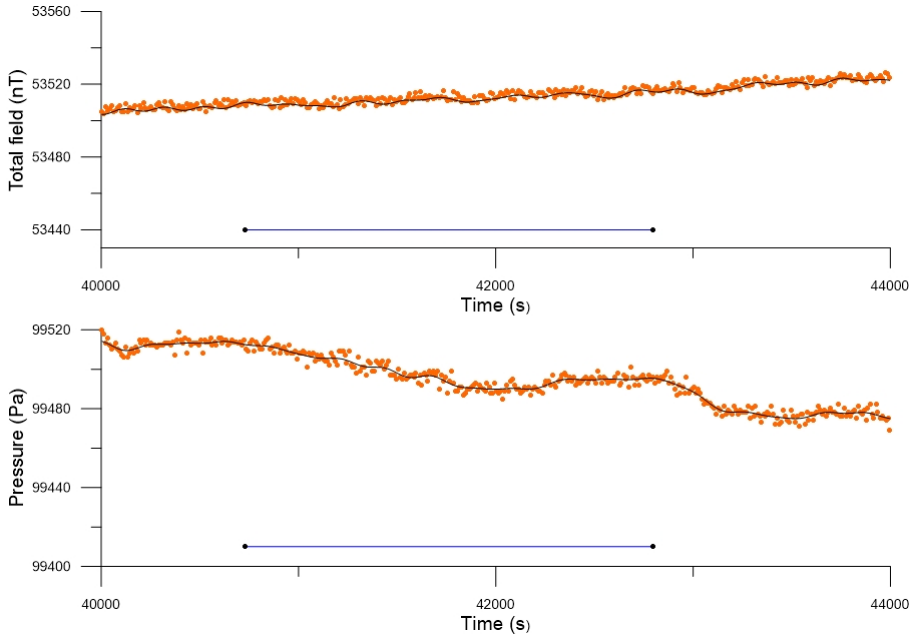

Figure 4.1. Magnetic total field (upper graph) and barometric pressure (lower graph) recorded at Ryssänlampi base station on March 5th 2016. The black line represents low-pass filtered data used in the base station correction. The blue lines indicate the duration of the flight F1. Horizontal axes show the time in seconds from midnight (UT).

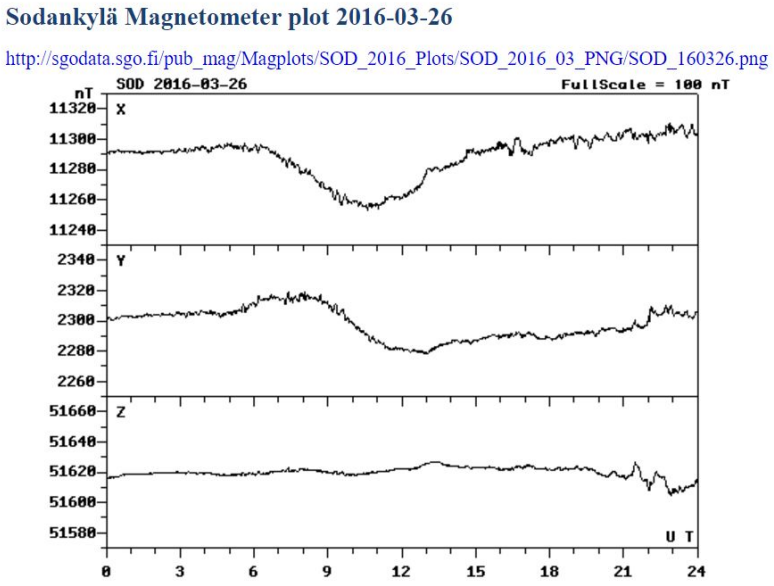

Figure 4.2. Geomagnetic activity (magnetic X, Y, Z components) measured by the Sodankylä observatory in March 26 2016. The amplitude change in geomagnetic is about ±20 nT.

5. Equivalent layer modelling (ELM)

Equivalent layer modelling (ELM) is used to grid the total field data at a constant elevation level using a numerical modelling of the data. The main advantage of ELM is that it removes effects of varying flight altitude and uneven sampling of the data points. In principle, ELM operates like a low-pass filter that removes features that cannot be modelled.

ELM is a process that begins with data harvesting, which reduces the number of data by discarding uninformative data points. Harvesting is necessary because the original total amount of data is usually so large that practical inversion would be impossible. In case of Ryssänlampi, data reduction was about 87% (from 33526 to 4255 points).

The next step in ELM is the generation of a 3D susceptibility model that consists of a single layer of rectangular prisms. In Ryssänlampi the horizontal size of the elements was set 25 m × 25 m and the vertical height was 250 m. The depth to the top of the model was 12.5 m and the terrain topography was not taken into account. Margin elements were added to the sides of the model to move the effects due to model edges away from the bordering data points. The total number of elements was 80×81 = 6561, but only 3090 of them were free in the inversion.

After setting up the data and the model, numerical inversion was used to optimize the susceptibility of the model elements in such a way that the synthetic response of the 3D layer model fits the UAV measured magnetic total field data. The forward computation is based on the solution for dipping magnetized prism by Hjelt (1972). The unconstrained inversion method has been described in Pirttijärvi (2003). The constrained inversion method, which aims to minimize the model roughness together with the data misfit, is based on the Occam inversion method used in Grablox2 software (Pirttijärvi, 2014b). The final model was obtained in 15 iterations using constrained inversion (QR+Occam). The final RMS-error computed from the radially weighted (R=200m) the data was about 3.78%.

The model obtained from the inversion was then used to compute the magnetic field on a constant altitude on a regular (25 m by 25 m) grid. The intensity and the direction of the inducing magnetic field were derived from IGRF field (B_0=53314.5 nT, I=76.93°, D=11.36°) computed using epoch 2016.2. After inversion, the response (X, Y, Z components and total field) was also computed at the original data locations and saved to processed UAV data file.

Figures 5.1a–5.1f show the fit between measured and modelled data in profile plot format. In general, the fit is rather good. The lowest minima and shortest wavelength anomalies are not fitted as well as the maxima, partially because of the size of the model elements (25 m by 25 m) and partially because some "negative" anomalies are caused by remanent magnetization that cannot be modelled with magnetic susceptibility alone.

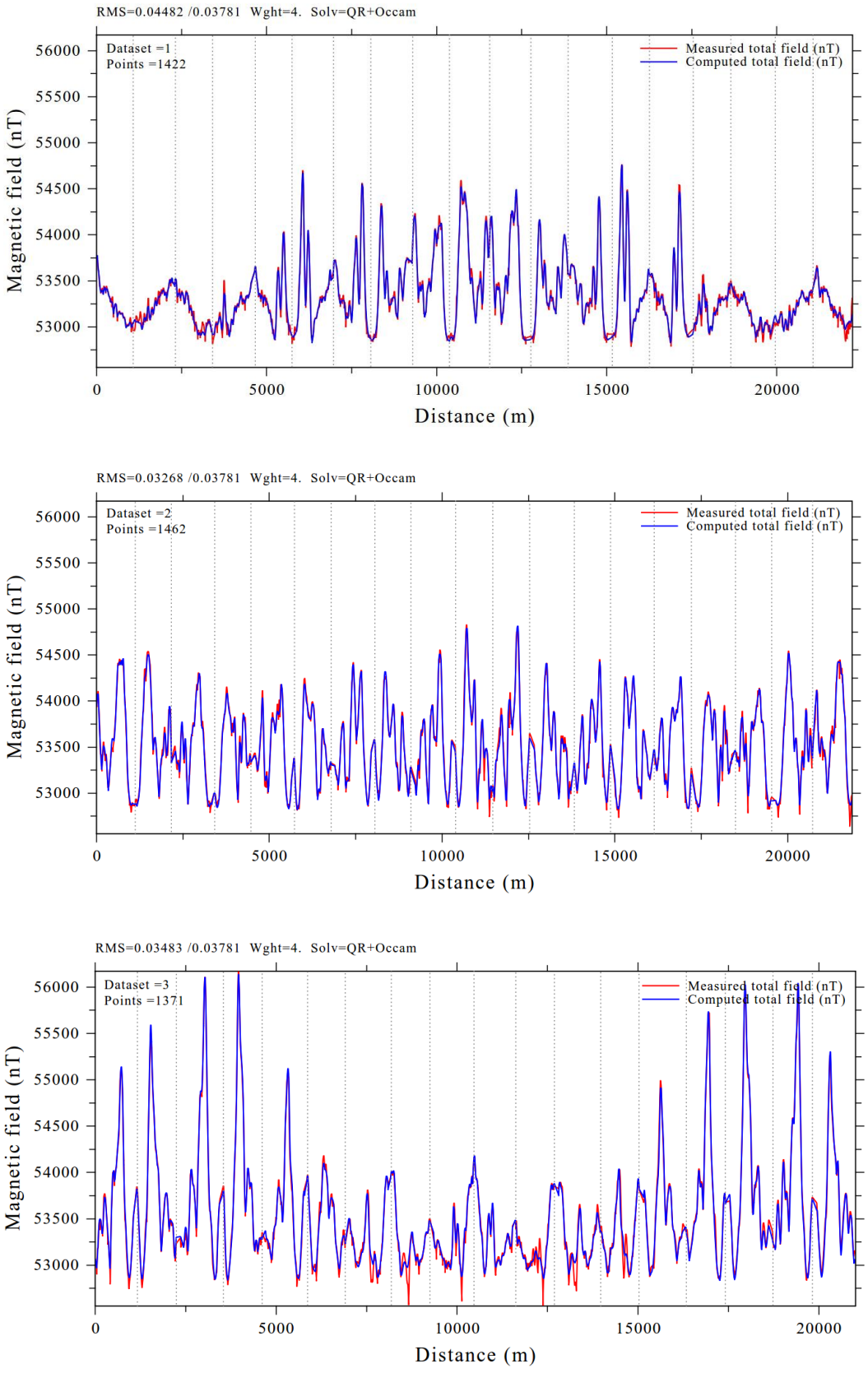

Figure 5.1. The fit between measured (red) and modelled (blue) magnetic total field for datasets F1 (top), F2 (middle) and F3 (bottom). The vertical dotted lines represent profile positions where the flight line turns around.

Figure 5.2 shows the measured and modelled data, the data misfit and the susceptibility model. To make the comparison easier, the color scale is the same in the first two maps. The range of the misfit is rather large (between -460 nT and +290 nT), but the mean and of the median are rather small being -0.43 nT and -3.15 nT, respectively. The standard deviation of the data misfit, 42.5 nT, could be considered as a measure of the noise in the data. Fig. 5.2 shows, however, that the biggest misfit is located near a magnetic minimum at the SE side of the survey area. The shape of the anomaly suggests that it is caused by remanent magnetization that ELM cannot model unless negative susceptibility values were allowed or the direction of the magnetization was taken into account. Therefore, in this case the misfit is not a good estimate of the level of noise in the data.

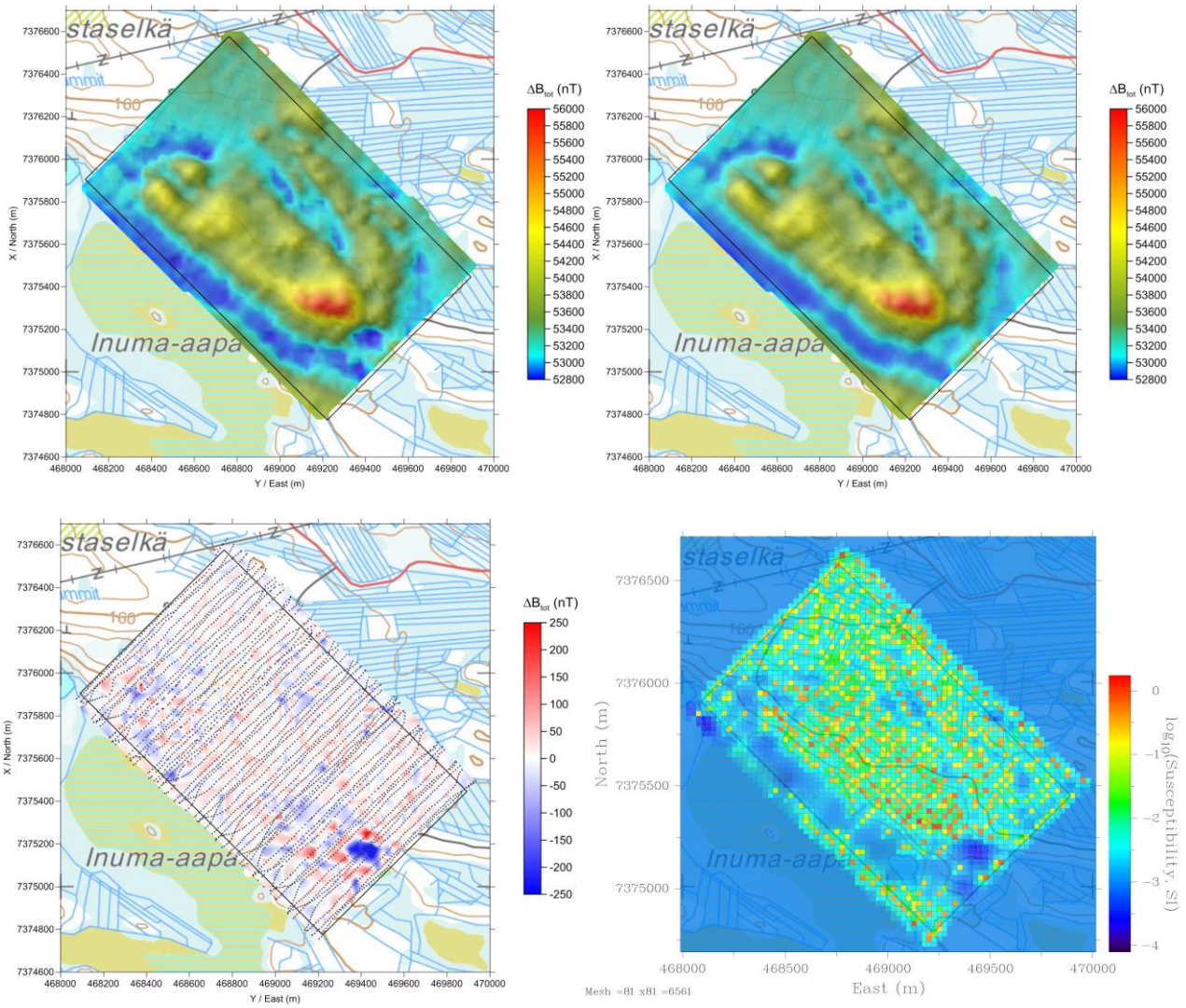

Figure 5.2. The harvested measured data (top left), computed total field (top right) and the difference between the two (bottom left) and the susceptibility model (bottom right) obtained from Ryssänlampi equivalent layer modelling (ELM). The distribution of the 4255 harvested data points are shown above the difference map.

6. Results

The results of Ryssänlampi magnetic survey are presented in digital format as:

a) A column formatted text file (*.UAV) containing the data at the original irregular data locations,
b) Three ESRI/ARC Ascii (ASC) grid files containing total magnetic field computed on an even grid (25 m x 25 m) on a constant height level of 0, 15 and 30 m above surface, and
c) A column formatted (XYZ) text file containing the magnetic field computed at the height of 0, 15 and 30 m at the same locations as GTK's ground magnetic data.

Some results are presented in Figs. 6.1-6.4.

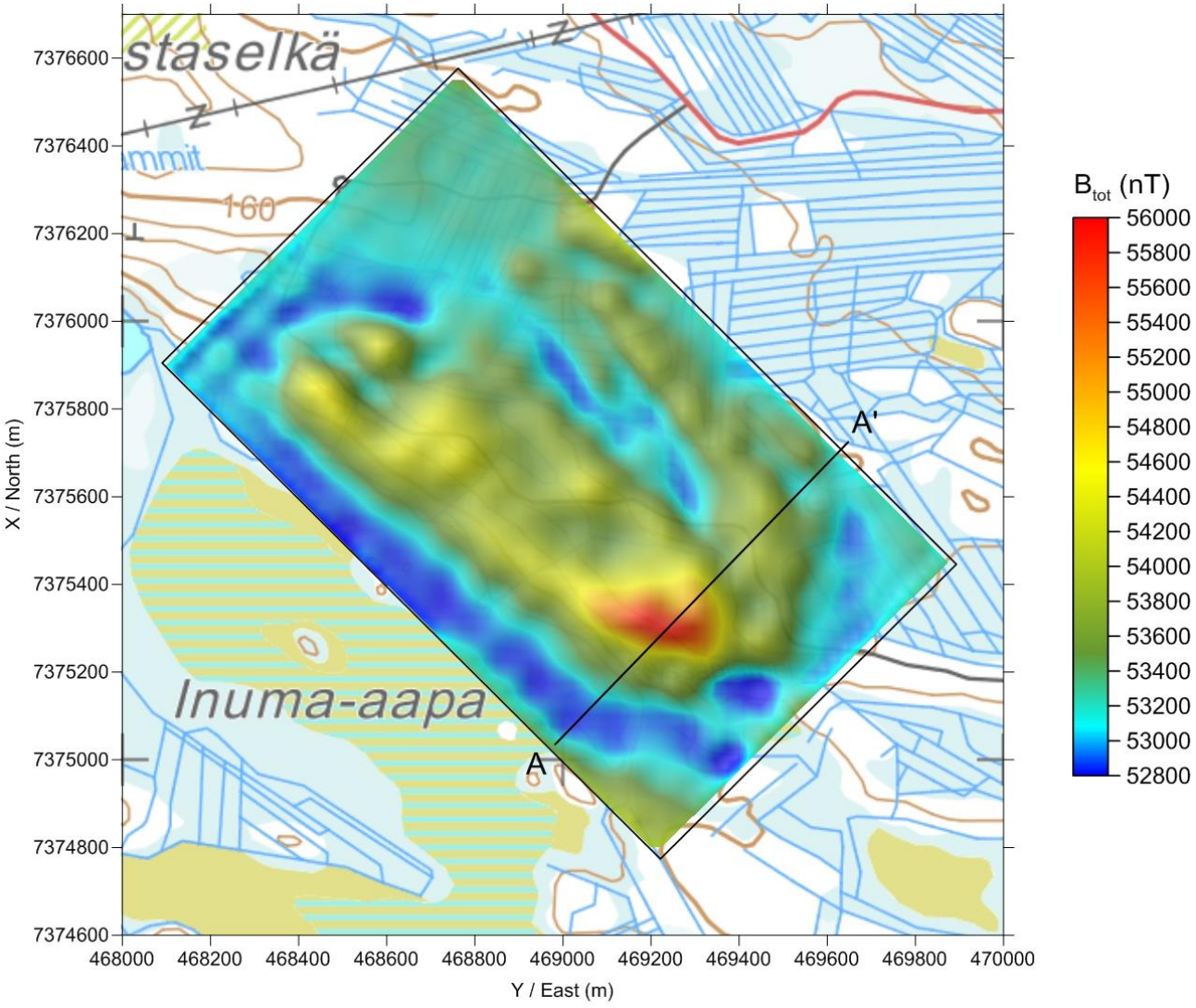

Figure 6.1. Map of corrected magnetic total field of Ryssänlampi site. The data are and low-pass filtered using cut-off wavelength λ=75m.

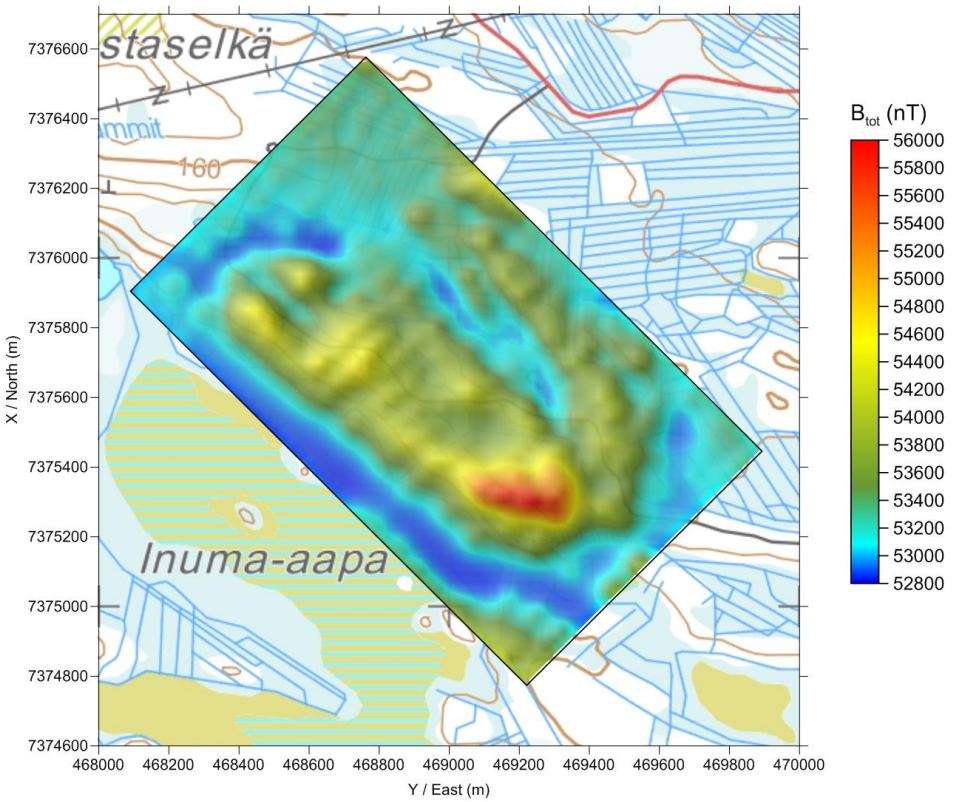

Figure 6.2. Map of magnetic total field of Ryssänlampi site computed at the constant height of 30 m using ELM.

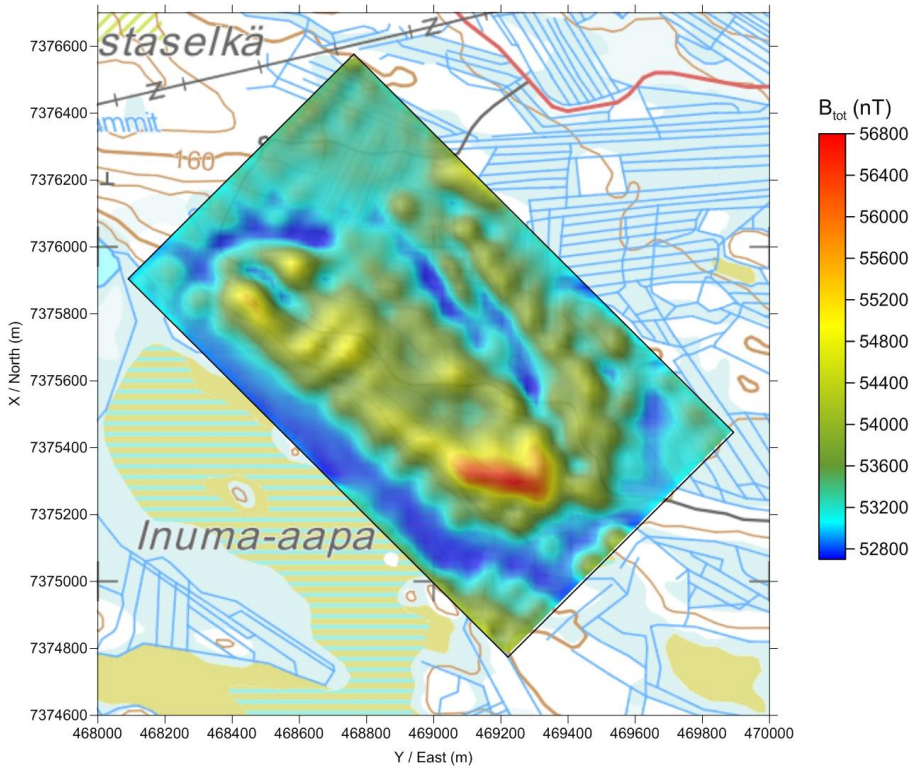

Figure 6.3. Magnetic total field of Ryssänlampi site computed at the height of 15 m using ELM.

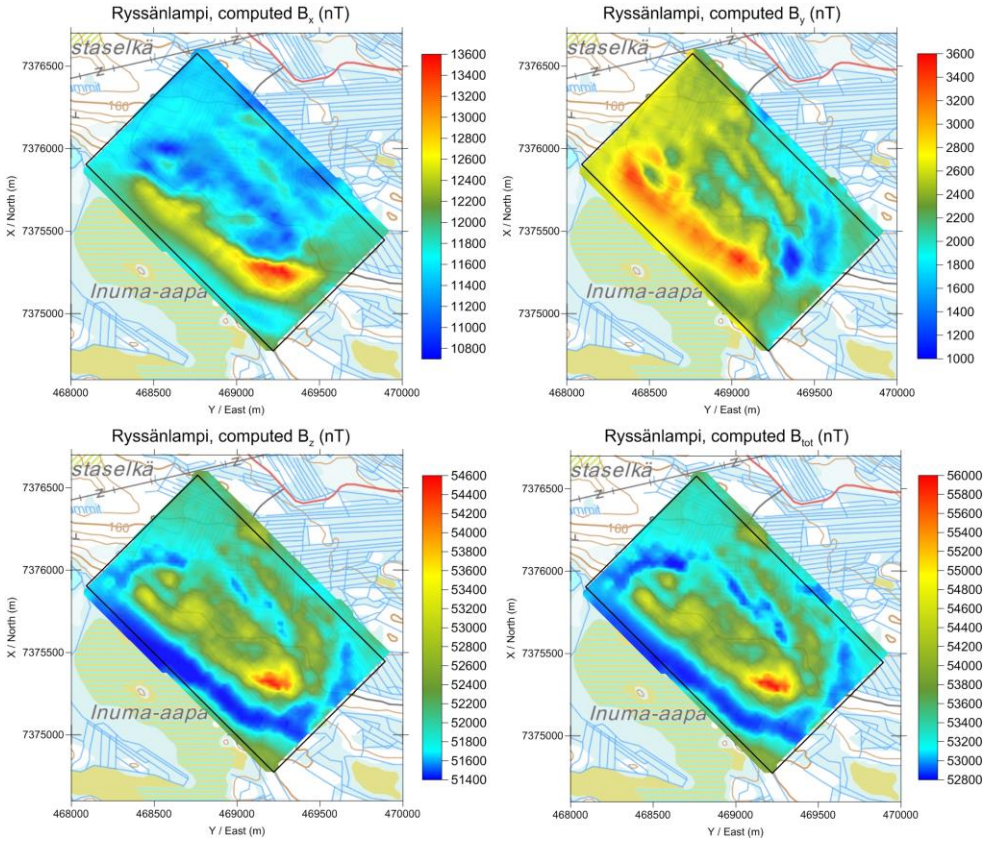

Figure 6.4. Synthetic X, Y, and Z components and total magnetic field of Ryssänlampi computed at original data locations. The XYZ components were computed from total field using the inclination and declination defined by IGRF (on 2016.2).

The processed data are saved in a special column formatted UAV text file format used by RadaiPros. An example of the file header and the first two rows are given on the next page (note that the lines are so long line that they continue on the next line).

The first line is a header line which defines the data. The second line defines the number of profiles (NPRO), total number of data points (NTOT), and file version number (VERS). The third line defines the decimal year of the measurements (YEAR) and the mean longitude (LON) and latitude (LAT) of the survey site. This information is used to compute the IGRF reference field. The fourth line contains on/off= 1/0 flags that define whether or not flight height has been corrected using DEM model (ALTI), or base station correction (BASI), or heading correction (HEDI), or tie-line levelling (TIEL) has been made.

The next five lines are defined separately for each dataset (survey flights). The first one (fifth line) defines the number of points (NPTS) and the index number of the dataset (I). The next line defines the base pressure (BASEP), and the x and y coordinates (XBP, YBP) of the reference point used to define the heights from the ground surface. The next line defines the intensity of the total field (CALIB) and the x and y coordinates (XBC, YBC) of the reference point used in fluxgate calibration. The next line defines the amount of heading correction along the two principal directions of the flight lines (HEAD1, HEAD2) and the leveling (LEVEL) obtained from heading correction.

Ryssäntalvi

3 33523 0.73 ! NPRO, NTOT, VERS

2016.2 26.29200 66.50500 ! YEAR, LON, LAT

1 1 2 0 ! ALTI, BASI, HEDI, TIEL

12647 1 ! NPTS, Ith

101024.0 468491.6 7376327.0 ! BASEP, XBP, YBP

53336.0 7376319.0 468515.0 ! CALIB, XBC, YBC

8.8 5.5 0.0 ! HEAD1, HEAD2, LEVEL

2016 3 5 ! YEAR, MONTH, DAY

Time Pres Roll Pitch Yaw Temp Curr QC Lon Lat Alt1 RawX RawY RawZ RawT X_TM25 Y_TM35 Alt2 Topo Dist Azim MagB Head CorX CorY CorZ CorT ComX ComY ComZ ComT HeaX HeaY HeaZ HeaT

40865.76 99090.0 6.10 -0.51 -157.61 20.90 9.89 3 26.29803 66.50726 30.00 -15575.326 -2289.912 51471.344 54021.430 468774.7 7376628.5 190.06 160.07 0.00 -148.64 0.01 -0.92 15081.459 2741.774 51554.895 53738.492 10939.979 2513.087 52575.980 53782.383 1.126 0.226 4.947 5.078

40865.88 99092.0 6.08 -0.96 -157.90 20.90 9.88 3 26.29800 66.50725 30.00 -15930.005 -2382.701 51349.531 54015.543 468773.4 7376626.5 190.08 160.08 2.34 -144.46 0.01 -0.95 15114.639 2741.768 51554.758 53747.336 10974.971 2544.292 52594.438 53786.633 1.157 0.233 5.084 5.219

…

The text string contains labels of each data column. The data columns are: 1= decimal time in seconds from the midnight (UT), 2= pressure (Pa), 3= roll (°), 4= pitch (°), 5= yaw (°), 6= temperature (°C), 7= current (A) fed to the engine, 8= GPS signal quality (from 0= no GPS to 3= excellent), 9 and 10= longitude (°) and latitude (°), 11= height (m) from the ground or altitude (m) from the reference point depending if altitude correction has been made (ALTI=1) or not (ALTI= 0), 12-15= raw X, Y, Z component and total magnetic field (nT), 16 and 17= X (east) and Y (north) rectangular coordinate (m) of the data point (Finnish ETRS-TM35FIN system), 18= altitude from the sea-level (m), 19= elevation of the topography (m) from sea-level, 20= cumulative distance (m) from the first point of the dataset, 21= azimuth (°) of the flight path (positive east from north), 22= base station correction of the total magnetic field (nT), 23= heading correction factor, 24-27= corrected X,Y and Z components and total magnetic field (nT), 28-31= computed X, Y and Z components and total magnetic field (nT), 32-36= heading and levelling corrections (nT) on X, Y, Z component and total magnetic field.

7. Comparison to existing magnetic data

GTK has carried out a ground magnetic survey at the Ryssänlampi area in January 2014 using a proton precession magnetometer and line spacing of 50 m (SW-NE directed lines). In summer 2015 Radai Oy made the first magnetic UAV survey at Ryssänlampi (Pirttijärvi, 2015). In the following, the results of the new UAV survey are compared to existing data. All example maps have been prepared using Golden Software Surfer version 13 and minimum curvature interpolation method on a grid size of 25 m by 25 m.

Figure 7.1 compares GTK's ground magnetic data with Radai's magnetic UAV data computed on the ground level using ELM. For easier comparison, both datasets have been low-pass filtered using Fourpot 1.3 software (Pirttijärvi, 2014b). The color scales of the two maps are the same, but the levels are adjusted to account for the time-dependent (2 years) difference in the magnetic field levels. The general shapes on the anomaly maps are much alike and the anomaly amplitudes are comparable. Radai's data shows more short-wavelength variations indicating that the original data is noisier.

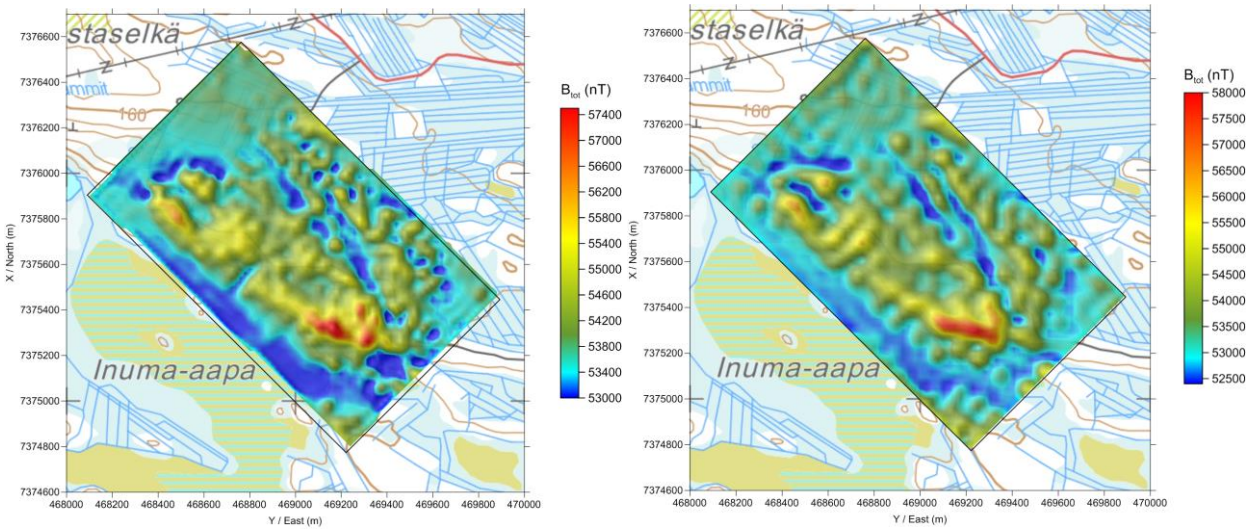

Fig. 7.1. Comparison between GTK's ground magnetic data (left) and Radai's (low-pass filtered) magnetic UAV data computed on the ground level z= 0 m using ELM (right).

Figure 7.2 compares GTK's upward-continued ground magnetic data with Radai's magnetic UAV data computed using ELM at the same height level of 30 m above ground. For better comparison Radai's data has been low-pass filtered. The upward-continuation and low-pass filtering was made using Fourpot 1.3 software (Pirttijärvi, 2014b). Like before the color scales of the two maps are the same, but the levels are adjusted. The overall similarity of the two maps in Fig. 7.2 is better and the amplitudes of the magnetic anomalies are closer to each other than in Fig. 7.1. The shape of the SW-NE directed profiles interpolated across the main anomaly are quite similar.

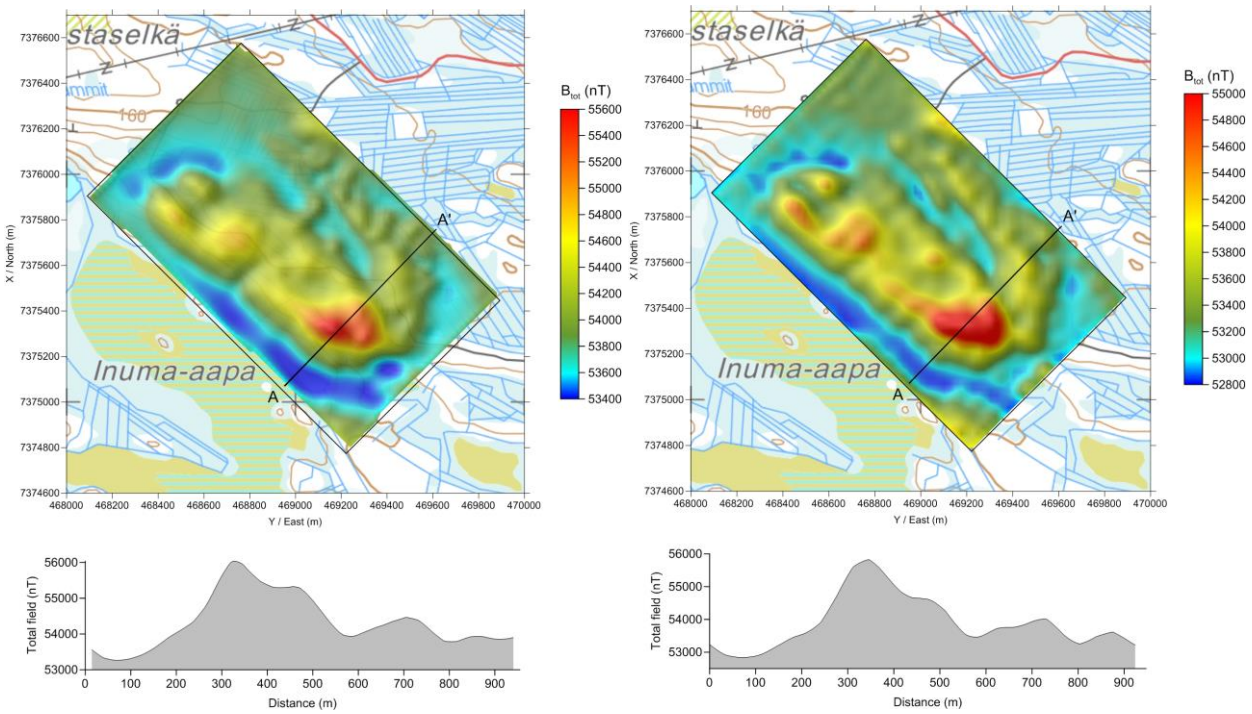

Figure 7.2. Comparison between GTK's ground magnetic data upward continued by 30 m (left) and Radai's corrected magnetic data (right). The profile graphs are interpolated along the SW-NE directed lines A-A' across the main magnetic anomaly.

Fig 7.3 compares Radai's new UAV based magnetic survey with the old survey (Pirttijärvi, 2015) recomputed using ELM on a constant altitude level of 30 m. The same color scale and levels are used in both maps. The maps and especially the profile sections are very similar but the new survey brings up more details. The three reasons for this are: 1) lower flight altitude (30 m instead of 40 m), 2) finer discretization of the susceptibility model (25 m by 25m instead of 40 m by 40 m) and 3) enhanced nominal line spacing (30 m instead of 50 m).

The improvement in data quality is perhaps even clearer when looking at the corrected data in Fig 7.4. In the old survey, the equivalent layer modelling (40 x40 m element size) was used to clean up measured data. In the new survey the corrected data (Fig. 7.4) and ELM computed data (Fig. 7.3) are much more alike and the amount of "stripes" is less than when comparing the old corrected and old modelled data with each other. Because the striped features are still visible in the raw magnetic data (Fig. 3.6), the improvement is mainly due to better data calibration. Another reason could be the use of a dedicated orientation sensor instead of the autopilot. Please, note that the sun shading is used in all figures to bring up the small details. Without sun shading the differences would be hard to see.

In terms of data quality the magnetic winter survey was successful despite the problems with flight operations, instrumentation and base station operation. Comparisons to old survey (Pirttijärvi, 2015) show that Radai's new UAV based magnetic surveying system provides enhanced data quality.

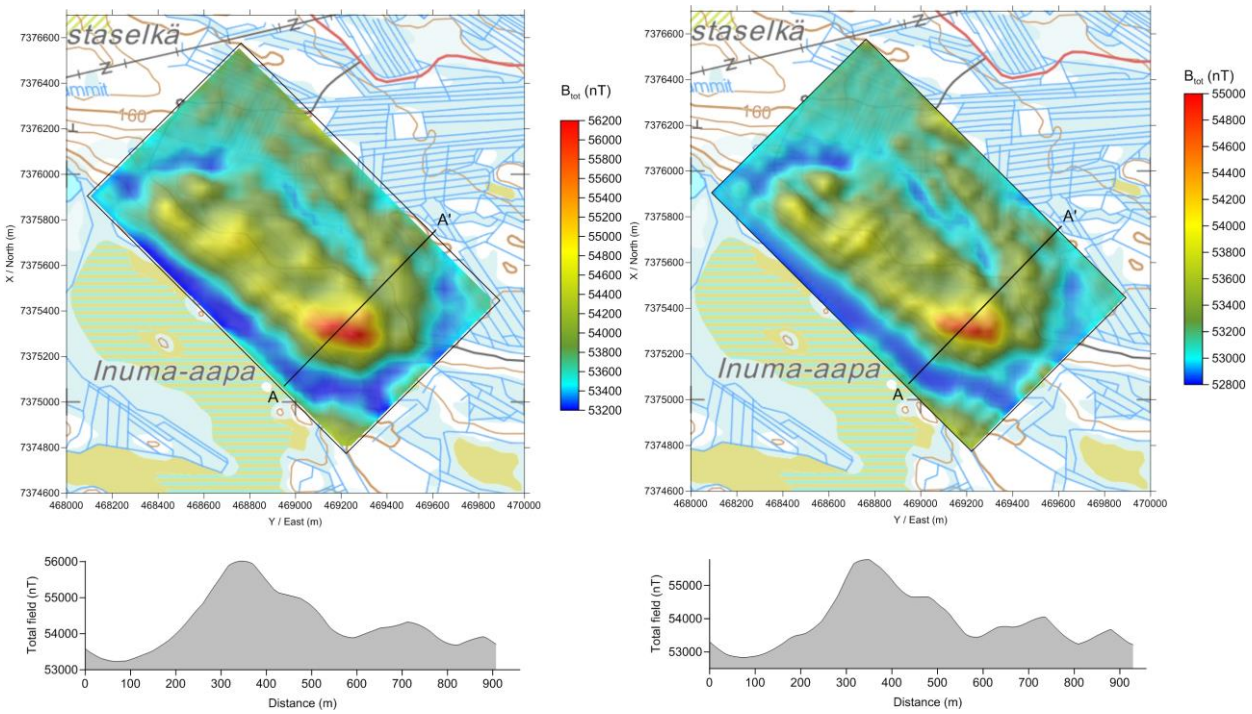

Figure 7.3. Comparison between Radai's old (summer 2015, on the left) and new (winter 2016, on the right) magnetic UAV data computed at the height of z= 30 m using ELM. The profile graphs are interpolated along lines A-A'.

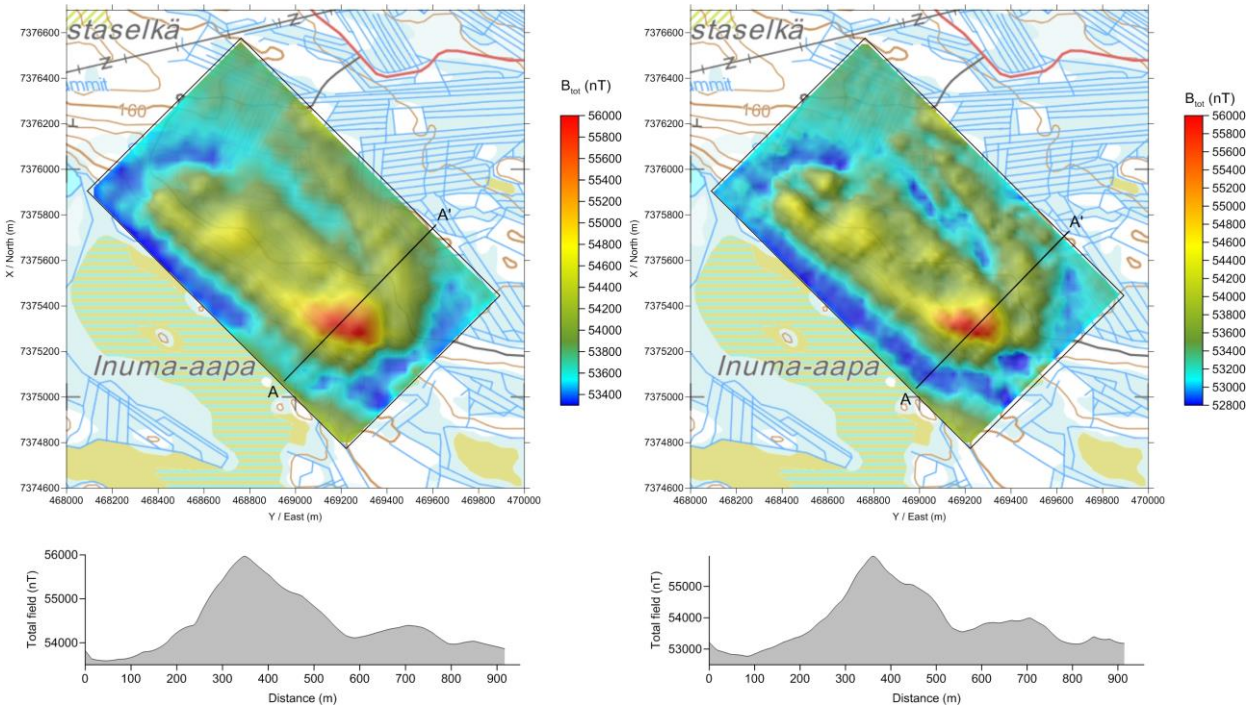

Figure 7.4. Comparison between Radai's old (summer 2015, on the left) and new (winter 2016, on the right) corrected magnetic total field data. The amplitude levels are different due to different flight height (40 m vs. 30 m). The profile graphs are interpolated along the lines A-A'.

8. The role of winter conditions

One of the main purposes of this study was to test the UAV based magnetic surveying system in winter conditions. On February 12th (campaign C1) the temperature was -3 – -1° C, wind was blowing about 2–5 m/s from N to NE. Wet snow was raining most of the day and the visibility was poor. On Feb 13th the temperature was about the same, dry snow was falling during the first half of the day but visibility was a little bit better than the day before. The wind was blowing about 1–2 m/s from SE. About 10-15 cm of new snow had rained during the night, the roads had not been cleared but they could be still driven on. On both days a covering tarpaulin had to be spread over the backside of the mobile control station to provide shelter for the equipment (cf. Fig. 8.1). The weather station had to be covered too.

On March 5th (campaign C2) the temperature was about -5°C and the wind was blowing 2–4 m/s from east. Dry snow was falling during the first half of the day but the visibility improved later that day. On March 6th the weather was clear and the visibility was good. The temperature was about -2–0°C and the wind was blowing 1–2 m/s from E to SE.

On March 26th (campaign C3) the temperature was 0 – +2°C, the wind was blowing 2 m/s from south (gusts 6 m/s), the weather was cloudy but the visibility was good because it was not snowing. As such, the conditions were moderately good for EVLOS operations.

Figure 8.1. Arto Karinen has put a tarpaulin over the back of Radai's mobile control station to give shelter from falling snow on February 13th. Photo by M. Pirttijärvi.

Figure 8.2. Ari Saartenoja is throwing and Christian Wieser is manually piloting Radai's Terrain Scout UAV in its take-off on February 12th 2016. Photo by M. Pirttijärvi.

All in all, the weather conditions were not very cold during any of the campaigns (min. -5°C). The prevailing temperatures did not seem to affect flight operations (piloting and telemetry) or the performance of UAV and measurement devices. Nonetheless, several observations can be made about winter conditions:

1. Snow was found the most problematic for various reasons.
    a. Falling snow decreases visibility more than equivalent amount rainfall making EVLOS operations impractical. The BVLOS operation mode is essential if the date of the measurements cannot be chosen based on good weather. The signal quality of the telemetry link was good despite the snowfall. Moreover, snow gets stuck on the UAV putting weight on it, and thus, requires brushing and cleaning before take-off. During take-off and flight the snowfall did not cause any problems.
    b. Melting snow turns into water, which does not play well together with electrical circuits and instruments. Extra care had to be taken to prevent snow entering the UAV chassis.
    c. In case of an emergency crash, the UAV has to be collected from the crash site. During campaign C1 the thickness of the snow cover was about 65 cm and the snow was very soft. Walking in the snow was tiresome even when using snow shoes. In campaigns C2 and C3 the snow was compressed so that skiing walking with snowshoes was easier. The size of the survey site was so small that there was no real need for a snowmobile (ski-doo). Besides, the use of a snowmobile outside official tracks requires permission from Metsähallitus (Administration of Forests). The permissions need to be applied in advance and cost 50-100 euros[1].

[1] http://www.eraluvat.fi/maastoliikenne/muu-maastoliikenne.html

   d. The cover behind the van provided an extended working place for many operations. Handling the UAV safely, however, required even more space than the cover could provide. Moveable shelter, similar those used in gardens, and covering an area of 3 m by 3 m could have been useful.
   e. On the good side, snow cover prevents or at least decreases the possible damages on the UAV in crash landing. Moreover, locating the (green) UAV from the approximate crash site provided by the SMS/GPS based locating system is easier from the snowy forest than it is from vegetated forest in the summer.
2. Although the cold was found a lesser problem, it affected UAV operations too.
   a. In cold conditions the batteries tend to worn out faster under load than in warm environment. To ensure c. 30 km long flight paths we added an extra battery inside the UAV chassis. Although, the Terrain Scout did handle the extra weight in normal flight, two problems came into being. First of all, the take-off became more demanding and required full throttle and the help of a co-pilot (cf. Fig. 8.2). Secondly, because the UAV speed was increased to provide additional lift (buoyancy), the turning radius increased and the sensitivity and capability of the UAV to follow the dense flight paths decreased.
   b. Heating up the batteries before the flight was found advantageous. The otherwise negative effect of self-heating while the battery discharges now became now an advantage. Special attention was paid on the voltage of batteries during flight. Had the weather been colder we could have estimated the decrease in the efficacy of the batteries better.
   c. The cold affects the human dexterity and the capability to perform simple tasks with fingers. If the temperature had been colder, extra trouble would have been experienced due to stiff fingers. The cold also affects the plastic/rubber insulation of electric wires. One must pay special care not to break the insulation of the cables. Another problem was also that tapes (electrical & duct tapes) tend to lose their gluing properties in cold and wet.
3. The safety of the working environment requires more attention in winter. For example, working in the same spot for a long time makes the ground icy and slippery. Warm, preferably waterproof working clothes and warm boots with rugged shoe soles are a necessity.
4. In bright winter daylight the computer screens and LCD displays are difficult to read. The backlight needs to be set to its maximum even when working in the shadows of the van and tarpaulin.
5. We used the van to get electricity for computers and battery charging. Keeping the car engine running during the time of survey is not friendly to the environment. Moreover,
6. In Finland, the so-called "every-man's right" does not permit making an open campfire without the permission of the landowner. Metsähallitus, however, allows making campfire in Lapland as well as Northern Ostrobothnia, Kainuu and North-Carelia[2] . A fire beside the control station gives not only a place to warm up and grill sausages, for example, but it also gives psychological comfort. Making a fire in winter is also safer than in summertime. However, in practice it requires that dry fire wood is brought along.
7. During deep winter (February-April) most of the forest roads are covered with snow that can make it impossible to reach the vicinity of the survey site. Lucky for us, Metsähallitus was logging near Ryssänlampi and kept the roads open. However, because of the ploughed snow the roads are much narrower and finding a safe place for the control station is more difficult than it is in summertime.

[2] http://www.metsa.fi/tulenteko-ja-puunottoluvat

Figure 8.2. Radai's UAV performing magnetic surveying in Ryssänlampi on February 13th 2016. Photo by M. Pirttijärvi.

9. BVLOS operation mode

Civilian UAVs are relative new participants in the airspace. As such, regulators and operators are still looking for safe and efficient use of these unpiloted aircrafts. Presently, every country has its own regulations. In Finland, the basis is the aviation law 864/2014[3] and specifically directive OPS-M1-31[4], which deals with UAV operations. UAVs must not endanger humans on the ground, airplanes, parachutists or any other air participants. All flights have to be observed by the pilot (visual line-of-sight – VLOS) or by an observer (extended line-of-sight – EVLOS). For BVLOS (beyond visual line-of-sight), the airspace must be closed during flights, as the principal anti-collision rule "see and avoid!" cannot be performed by the UAV pilot.

Radai applied for BVLOS permission from Trafi for the Ryssänlampi survey on 10.12.2015. The permission was granted on 31.12.2015 for a two-week period from 8.-19.2.2016 and for a height up to 1400 feet. The permission cost 320 euros. The reserved area (Fig. 9.1) is significantly larger than the actual survey area, as the UAV must never leave it. To ensure this, we geo-fenced the survey area in multiple ways: 1) pilot can stop the motor and activate the vertical landing system, 2) autopilot returns the UAV to the starting point (control station) if it recognizes a geo-fence breach, and lastly 3) an independent system terminates the flight. This effort is justified, as the UAV could interfere with the air traffic of Rovaniemi airport or the nearby reserved military air space.

[3] http://www.trafi.fi/filebank/a/1415795417/65aac65181cc2fd47eb2b6c950b2c8b0/16189-Laki.pdf
[4] http://www.trafi.fi/filebank/a/1364306591/ab5c5aafa44cd1081458ab56d3c94f2f/11861-OPS_M1-31.pdf

After consultation with Trafi and Finavia, new permission was granted for the same airspace for a period from 5.- 8.3.2016 (campaign C2). However, the third request for campaign C3 on 25.-28.3.2016 was denied by the Air Management Center (AMC), citing a new risk assessment, which had not been communicated with us. According to Finavia representative "The process according to Finnish aviation act for establishing a danger area by AMC (Airspace management Cell) is still work in progress and is not official yet". We hope the procedures become established in the near future, as BVLOS enables safer and more efficient operation mode for UAV based geophysical surveys.

Regarding the magnetic survey at Ryssänlampi, the BVLOS operation mode was found superior compared to EVLOS mode. BVLOS permit allows performing UAV operations without visual line of sight to the UAV and hence enables surveying larger areas more cost-effectively.

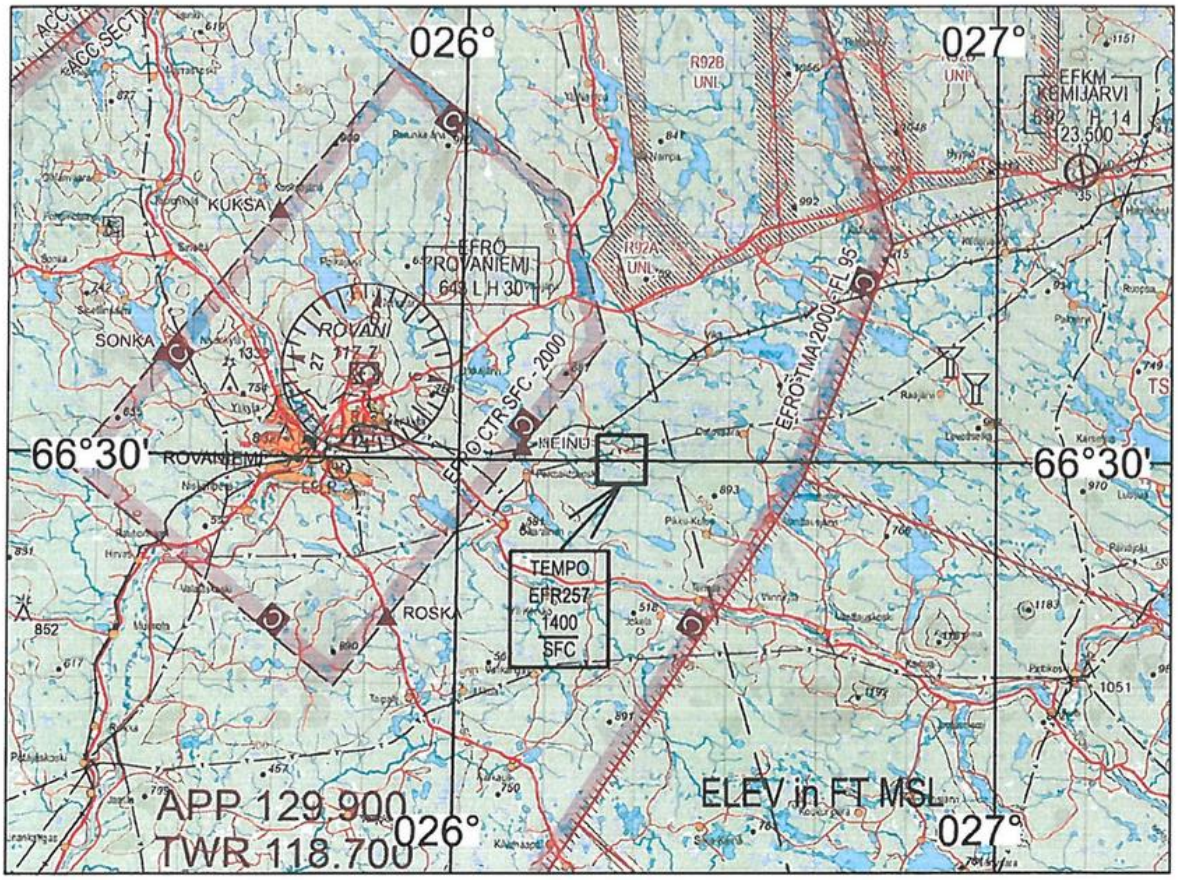

Figure 8.2. The location of the reserved air-space (black rectangle), the air space of Rovaniemi airport (purple polygon west of Ryssänlampi), and reserved military air space (red polygons north of Ryssänlampi).

10. References

Hjelt, S.-E., 1972. Magnetostatic anomalies of dipping prisms. Geoexploration, 10, 239-254.

Merayo, J.M.G., Brauer, P., Primdahl, F., Petersen, J.R. & Nielsen, O.V., 2000. Scalar calibration of vector magnetometers. Meas. Sci. Technol., 11, 120-132.

Pirttijärvi M., 2003. Numerical modeling and inversion of geophysical electromagnetic measurements using a thin plate model. PhD thesis, Acta Univ. Oul. A403, Univ. of Oulu.

Pirttijärvi M., 2014a. FOURPOT - Potential field data processing and analysis of using 2-D Fourier transform; User's guide to version 1.3a, University of Oulu, 54 pp < https://wiki.oulu.fi/x/0oU7AQ>.

Pirttijärvi M., 2014b. GRABLOX2 - Gravity interpretation and modelling using 3-D block models; User's guide to version 2.1, University of Oulu, 63 pp < https://wiki.oulu.fi/x/jYU7AQ>.

Pirttijärvi M., 2015. Ryssänlampi magnetic survey using Radai UAV system and its comparison to airborne and ground magnetic data of GTK. Detailed Survey Report, 21.8.2015, Radai Oy, 26 pp. <http://tupa.gtk.fi/raportti/arkisto/73_2015.pdf>